Processing and Application of Ceramics 17 [4] (2023) 393–399
https://doi.org/10.2298/PAC2304393K

Giant dielectric properties of $CaCu_3Ti_4O_{12}$ ceramics synthesized by solid state reaction route

AP Kajal Parida, Pawan Kumar*

Department of Physics and Astronomy, National institute of Technology Rourkela, Rourkela 769008, India

Received 4 May 2023; Received in revised form 4 October 2023; Accepted 30 November 2023

Abstract

$CaCu_3Ti_4O_{12}$ (CCTO) ceramics were prepared by solid-state reaction route, calcination at 1050 °C for 4 h and sintering at 1050 and 1100 °C for 8 h. X-ray diffraction and Raman studies of the CCTO powders and sintered samples confirmed the formation of single phase cubic structure with small amount of CuO in the sintered ceramics. Scanning electron microscope study revealed the average grain size between ~6 µm to ~29 µm in the CCTO ceramics sintered at 1100 °C. Room temperature giant dielectric constant (ε_r) of the order of ~10^5 with relatively low dielectric loss at 100 Hz frequency was obtained in the CCTO ceramics sintered at 1100 °C. The present study has revealed that grain size plays an important role in enhancing the dielectric properties of CCTO ceramics.

Keywords: *$CaCu_3Ti_4O_{12}$, structure characterization, dielectric properties*

I. Introduction

Developments in the electronics industry, focused on creating multifunctional, intelligent, energy-efficient and miniaturized devices, have generated significant interest in the development of materials with excellent properties. One crucial component of electronic devices is the capacitor. The miniaturization of capacitor volume depends on the dielectric properties of the chosen material.

The perovskite-like $CaCu_3Ti_4O_{12}$ (CCTO) system has garnered the attention of researchers due to its large ε_r at RT (in the range of $\sim 10^3$–10^4 at 100 Hz) with excellent temperature stability in the 100–800 K range [1–4]. Various models, such as the surface/internal barrier layer capacitor (SBLC/IBLC), polaron-hopping, electron pinned defect dipole (EPPD) and non-ohmic sample electrode contact models, have been proposed to explain the excellent dielectric properties of the non-ferroelectric CCTO system [5]. In the literature, the IBLC model is predominantly used to explain the dielectric properties of CCTO-based systems. According to the IBLC model, polycrystalline CCTO ceramics can be considered as composed of semiconducting grains separated by thin insulating grain boundaries. In general, the value of relative permittivity is directly proportional to the grain size and inversely proportional to the thickness of grain boundaries. In CCTO system, oxygen vacancies, CuO segregation and aliovalencies of Ti and Cu ions play a crucial role in the formation of semiconducting grains and insulating grain boundaries [6]. According to the IBLC model, the dielectric properties of the system are quite sensitive to variations in processing conditions. Moreover, optimization of the processing temperature and the properties of a dielectric system depend on the chosen synthesis route.

Because of the potential applications of CCTO ceramics in multilayer capacitors, CCTO is prepared by using various synthesis techniques. Jesurani *et al.* [7] reported that CCTO ceramics synthesized by the sol-gel method exhibit ε_r of the order of 10^4. Mao *et al.* [8] reported the effect of grain size on the dielectric properties of CCTO ceramics and obtained ε_r of $\sim 3 \times 10^4$ at 1 kHz at RT. Zhao *et al.* [9] synthesized CCTO based powders with a surface coverage of nanosized TiO_2 particles to obtain giant dielectric properties. This suggests that the dielectric properties of CCTO system are dependent on processing parameters. Therefore, there is a need to study the effect of sintering temperature on the dielectric properties of CCTO ceramics.

In the present study, we have synthesized CCTO ceramics by using the conventional solid-state reaction

---

* Corresponding authors: tel: +91 0661 2463726,
e-mail: *pawankumar@nitrkl.ac.in*

route and effect of sintering temperature on the dielectric properties is studied in detail.

II. Experimental

Polycrystalline CCTO powders were synthesized by solid state reaction route. A stoichiometric amounts of precursors $CaCO_3$ (Merck, ≥98.5%), CuO (Merck, ≥99.9%) and TiO_2 (Merck, ≥99.5%) were thoroughly mixed via normal milling with zirconia balls, using acetone as the grinding media and ball-to-powder ratio of 3:1. The ball-milled powder was subsequently dried in an oven and calcined at 1050 °C for 4 h. To reduce brittleness and improve compactness among the powder granules, 3 wt.% of polyvinyl alcohol (PVA) was mixed with the calcined powder. Green pellets, with a diameter of approximately 10 mm and a thickness of ~1 mm, were obtained using a hydraulic press under a pressure of 60 MPa. The green pellets were sintered at temperatures of 1050 and 1100 °C for 8 h each and denoted as CCTO-1050 and CCTO-1100, respectively.

Structural study of the calcined powder and sintered pellets was performed by X-ray diffraction (XRD) on Rigaku Ultima IV diffractometer (Cu-K radiation, λ = 1.541 Å). Crystallite size (D) of the calcined powder was calculated by using Debye-Scherrer formula:

$$D = \frac{k \cdot \lambda}{\beta \cdot \cos\theta} \tag{1}$$

where k is 0.94, β is FWHM in radians, θ is the diffraction angle and λ is the X-ray wavelength used in XRD. Experimental density (ρ_{ex}) of the sintered samples was measured by using Archimedes principle using the formula:

$$\rho_{ex} = \frac{w_{dry}}{w_{soak} - w_{sus}} \cdot \rho_k \tag{2}$$

where $\rho_k = 0.81\,\text{g/cm}^3$ is the density of kerosene oil, w_{dry}, w_{soak} and w_{sus} are the dry, soaked and suspended weights of the sintered pellets, respectively.

Theoretical density of the CCTO system was calculated by using the below given relation:

$$\rho = \frac{n \cdot A}{V \cdot N_A} \tag{3}$$

where n is number of atoms per unit cell, A is the atomic weight, V is the volume of the unit cell and N_A is Avogadro's number (6.023×10^{23}).

Surface morphology of the sintered ceramics was studied with scanning electron microscopy (SEM, JEOL JSM-6480 LV) by using secondary electron beams. Dielectric properties at different frequencies and at different temperatures were measured by using LCR meter (Hioki 3532-50, Japan). Electrodes were prepared by deposition of silver paste on both sides of the sintered pellets and heating at 400 °C for 30 min in a muffle furnace for good adhesion. Vibrational properties were recorded by Raman spectrometer (WITec GmbH Model-XMB3000- 3000) by exciting samples with 532 nm laser light.

III. Results and discussion

3.1. Structural and density studies

Figure 1 shows XRD patterns of the calcined CCTO powder and sintered CCTO pellets. XRD patterns matched with JCPDS card no. 75-2188, which confirmed the formation of cubic perovskite CCTO phase with space group $Im\bar{3}$. However, along with cubic phase, some XRD peaks of a secondary phase were also observed in the sintered pellets. This secondary phase was identified as CuO phase (JCPDC card no 41-0254), which could be formed at higher sintering temperatures due to the diffusion of Cu at the pellet surface. Crystallite size of the calcined powder, determined by using Debye-Scherrer formula, was found to be ~9.1 nm. From Fig. 1, it can be clearly seen that with the increase of sintering temperature, the intensity of the XRD peaks increase, which suggest the increase of crystallinity of the sintered CCTO samples.

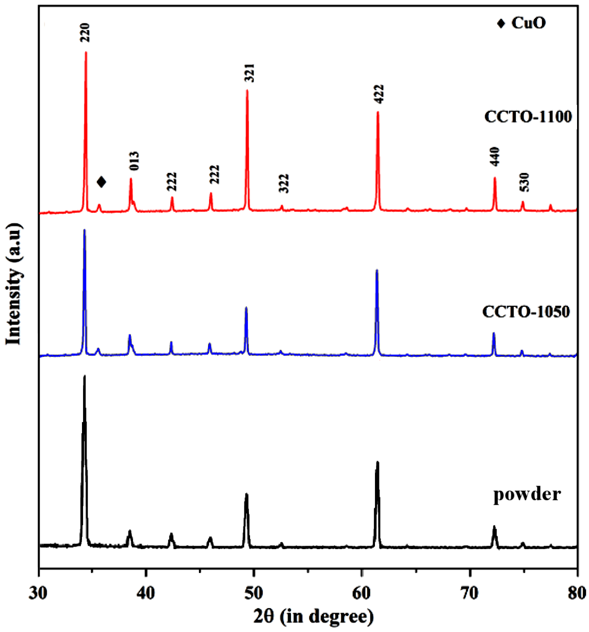

Figure 1. XRD patterns of calcined CCTO powder and CCTO pellets sintered at 1050 and 1100 °C

Experimental density of the CCTO-1050 and CCTO-1100 sintered pellets was found to be 4.23 and 4.79 g/cm^3, respectively. From JCPDS file 75-2188, the cell parameters of CCTO are considered to be $a = b = c = 7.3910$ Å and the number of atoms per unit cell is $n = 2$. Thus, theoretical density of the CCTO system, , calculated by Eq. 3, was found to be ~5.4 g/cm^3.

3.2. Raman study

The vibrational properties of the CCTO powder/sintered samples were studied by using Raman measurements, as shown in Fig. 2. Typically, Raman mode

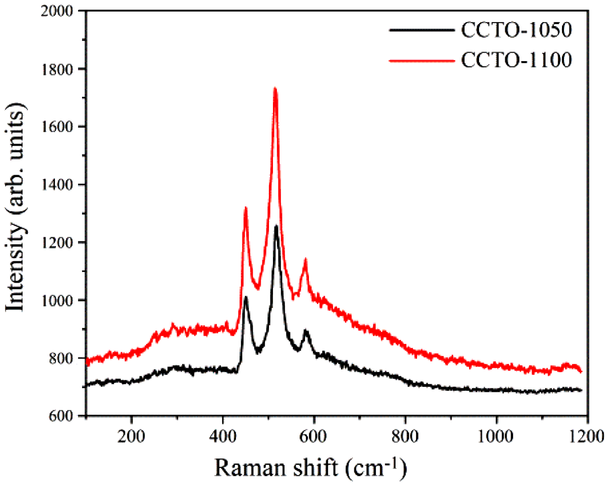

Figure 2. Raman spectra of CCTO-1050 and CCTO-1100 ceramics

frequencies in inorganic transition metal oxides are influenced by factors such as atomic symmetry, effective charge, bond lengths and atomic movements. Three prominent Raman modes in the wave number range of 400–600 cm^{-1} are characteristic Raman bands of CCTO ceramics [10,11], which are observed in spectra of both the CCTO-1050 and CCTO-1100 ceramics (Fig. 2). The observed Raman modes at ∼444 and ∼510 cm^{-1} correspond to TiO_6 rotation-like modes of the A_{g1} and A_{g2} bands, respectively. Additionally, the peak at 576 cm^{-1} corresponds to the F_{g3} band, responsible for the Ti–O–Ti anti-stretching mode of the TiO_6 octahedra [12,13]. These observed peak positions confirm that CCTO ceramics have a cubic perovskite structure. Furthermore, Raman modes for both the sintered ceramics remain unchanged, which is consistent with previous reports on CCTO ceramics [14,15]. The lack of significant changes in Raman modes may be attributed to the constancy of Ti-related lattice vibrations with variations in sintering temperature.

In addition, the intensity of Raman modes of the CCTO-1050 sample is comparatively lower than that of the CCTO-1100 ceramics. The higher Raman intensity of CCTO-1100 ceramics may be attributed to its relatively higher crystallinity. Raman mapping was conducted to further investigate the spatial variation of chemical composition of the sintered CCTO ceramics. Raman mapping covered both the grains and grain boundaries (GBs), enabling the clear observation of characteristic Raman modes. Figure 3 shows the Raman images (50 µm × 50 µm) centred at 444, 510, and 576 cm^{-1} for both the CCTO-1050 and CCTO-1100 sintered ceramics. Moreover, the GBs exhibit a characteristic Raman mode at ∼295 cm^{-1}, representing the A_g mode of the CuO phase [10,16]. It is evident that the Raman response of the CCTO-1100 ceramics is higher for all the Raman modes compared to the CCTO-1050 ceramics. The grain boundaries contain a lower proportion of CCTO phase compared to the grains. These spectroscopic findings are further supported by EDX analysis, which will be presented in the next section. The intensity variation across the grains corroborates the polycrystalline nature of the CCTO system [16]. Furthermore, when comparing the intensity of the Raman peak at ∼295 cm^{-1}, the amount of CuO phase on the grain boundaries of the CCTO-1100 ceramics is found to be higher than that of the CCTO-1050 ceramics.

3.3. Microstructural study

Microstructural analyses of both the CCTO-1050 and CCTO-1100 revealed the presence of bimodal grain size distribution (Fig. 4). The average size of small and large grains in the CCTO-1050 ceramics was calculated to be ∼8 and ∼28 µm. In contrast, the average size of small and large grains was found to be ∼6 and ∼29 µm in the CCTO-1100 ceramics. As mentioned earlier, not only the grain size but also the grain boundaries (GBs) play a major role to account the dielectric properties of sintered CCTO ceramics. Generally the grain boundaries

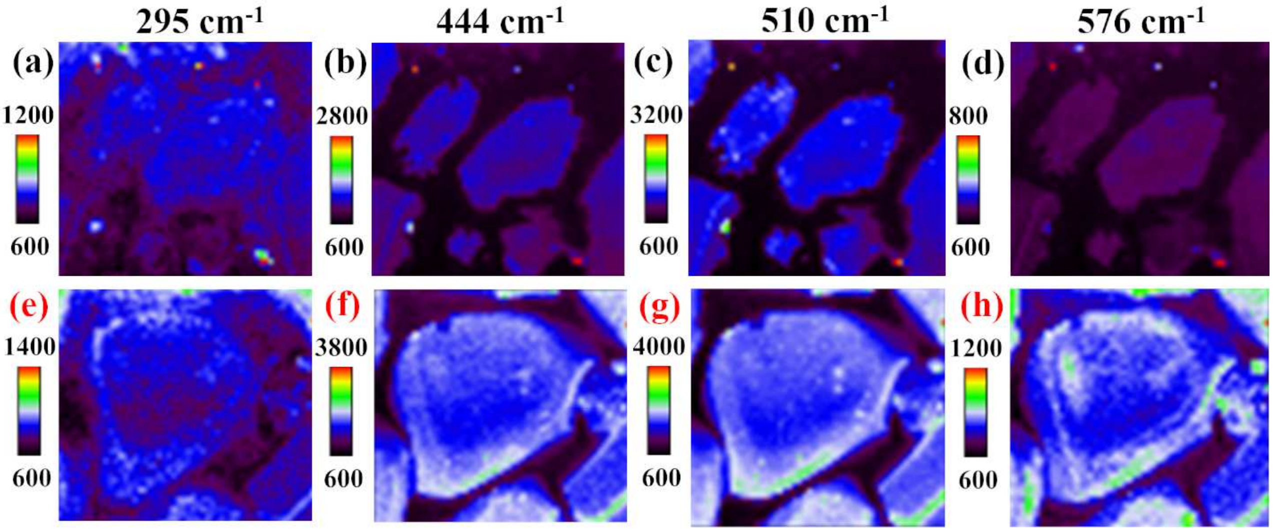

Figure 3. Raman intensity map of (a-d) CCTO-1050 and (e-h) CCTO-1100 ceramics (size of Raman scan regions are 50 µm × 50 µm)

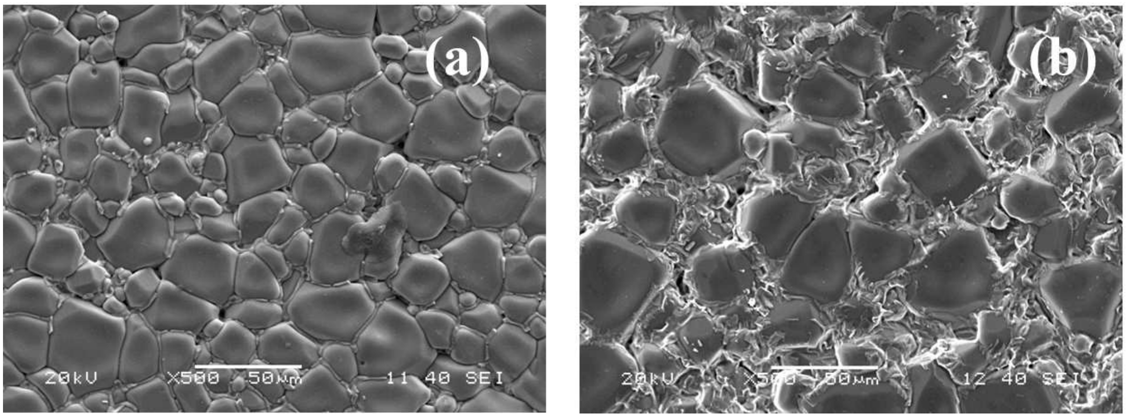

Figure 4. SEM micrographs of (a) CCTO-1050, and (b) CCTO-1100 ceramics

are comparatively less conducting than the grains. A melted-like topography is observed in the CCTO-1100 ceramics, which suggests that the melted-like phase is controlled by sintering temperature. At higher sintering temperatures, diffusion of Cu ions from lattice sites to the surface layer is the reason behind the stacking of melted-like phase in grain boundaries. Cu ions get oxidized to form the CuO phase at the GBs which results in the decrease of GBs thickness with the increase of sintering temperature.

Chemical composition of the sintered CCTO ceramics across the wide area, at discrete grains and at the grain boundaries are characterized by EDX (Figs. 5 and 6). In the CCTO-1050 ceramics, Cu/Ca ratio in the broad region, grain and melted phase was found to be 5.96, 2.88, and 10.26, respectively. In contrast, in the CCTO-1100 ceramics in broad region, grain and melted phase of this ratio was found to be 5.05, 2.84 and 40.39, respectively. Higher ratio of Cu content in grain boundaries of the CCTO-1100 ceramics can be attributed to the existence of more CuO phase at grain boundaries in the CCTO-1100 than in the CCTO-1050 ceramics. These calculated analytical results reconfirm the Raman results.

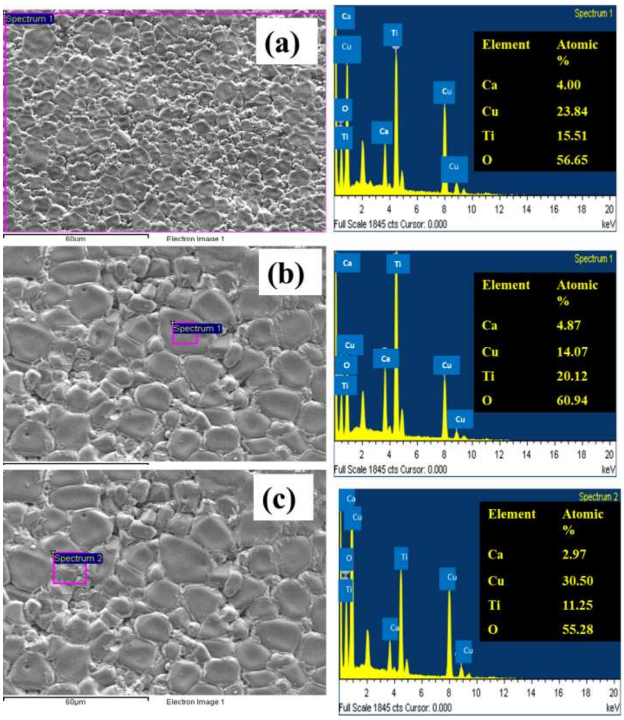

Figure 5. EDX spectra of: a) broad region, b) grain and c) grain boundaries of CCTO-1050 ceramics

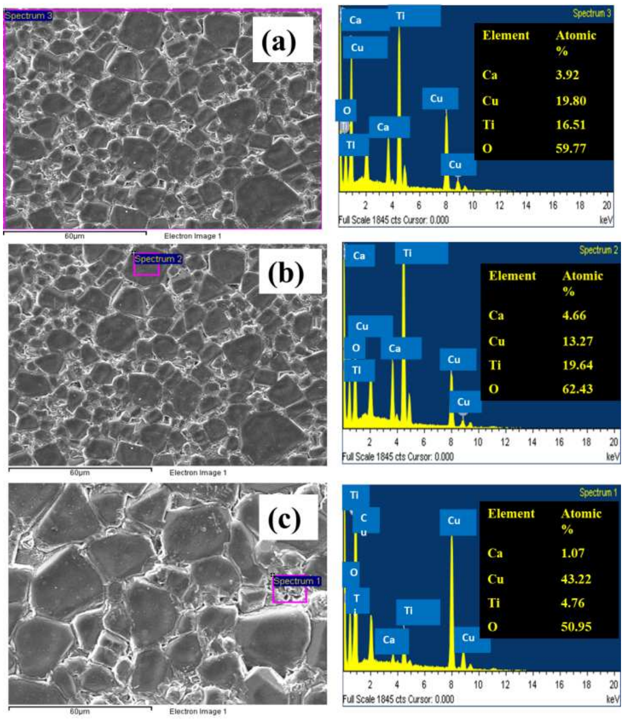

Figure 6. EDX spectra of: a) broad region, b) grain and c) grain boundaries of CCTO-1100 ceramics

3.4. Dielectric study

Variations of ε_r with frequency at room temperature of the CCTO-1050 and CCTO-1100 ceramics are shown in Fig. 7. Dielectric constants ε_r at RT for the CCTO-1050 and CCTO-1100 ceramics were 51611 and 139917 at 100 Hz, respectively. Observation of this relatively high ε_r values can be attributed to the larger average grain size of the CCTO ceramics, as suggested by the IBLC model. According to this model, the ε_r of the

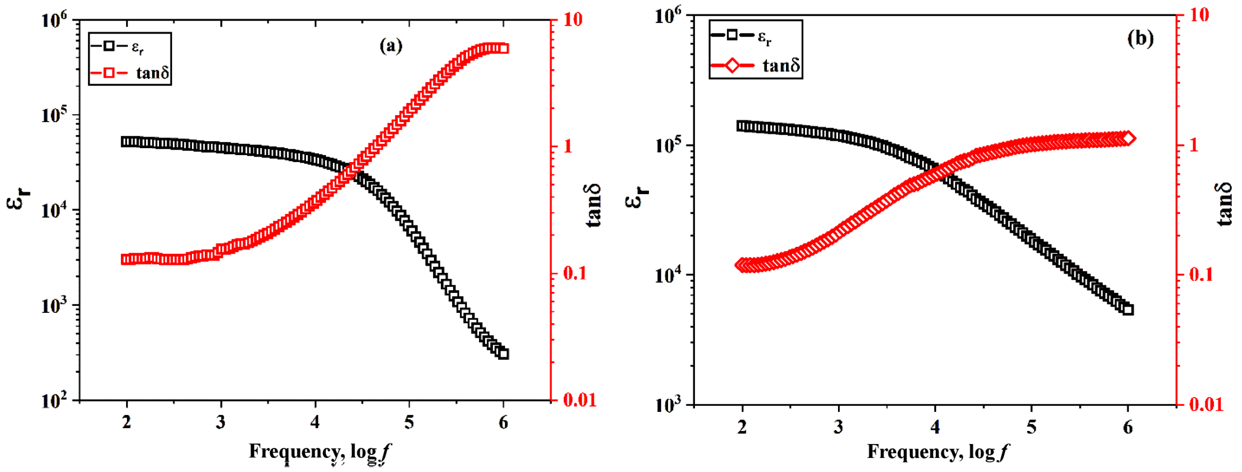

Figure 7. Variations of ε_r and tan δ with frequency for: a) CCTO-1050 and b) CCTO-1100 ceramics at RT

CCTO ceramics is directly proportional to the grain size and inversely proportional to the thickness of the grain boundary [17]. It has been observed that ε_r of all the ceramic samples decreases with the increase of frequency, a trend attributed to the corresponding reduction in net polarization [18]. High ε_r at low frequencies may be due to the space charge polarization, which occurs due to the accumulation of charges at the grain boundaries. Giant dielectric properties of the CCTO samples can be explained by the IBLC model, which suggests inhomogeneous microstructural composition in CCTO system, characterized by less resistant grains surrounded by more resistive grain boundaries. Grains act as conducting plates between the insulating grain boundaries, resulting in an increase in the total capacitance of the grains [19]. Furthermore, grain boundaries contribute to this effect by creating parallel capacitors within the CCTO samples. Microstructure and EDX results of the CCTO-1050 and CCTO-1100 ceramics (Figs. 4–6) indicate that grain boundaries are rich in the CuO phase, leading to the creation of insulating layers between the relatively conducting grains. Our findings align with the mechanism proposed by the IBLC model.

Temperature variations of ε_r and tan δ at different frequencies of the CCTO-1050 and CCTO-1100 ceramics are shown in Fig. 8. It was observed that ε_r at all frequencies remains relatively independent of temperature up to 130 °C. Above 130 °C, ε_r increases with the increase of temperature, specifically at 100 Hz and 1 kHz, while it remains relatively constant at 10 kHz, 100 kHz, and 1 MHz. RT dielectric loss (tan δ) of the CCTO-1050 and CCTO-1100 ceramics was found to be ~0.12 and ~0.11 at 100 Hz, respectively. Values of tan δ increase with the increase of frequency in both ceramics. This suggests the presence of dielectric relaxation process in theses ceramics samples [20].

Besides the requirement of excellent dielectric properties, relatively low temperature coefficient of capacitance (*TCC*) is an important requirement for electrical device applications and can be calculated by the following equation:

$$TCC = \frac{C_T - C_{RT}}{C_{RT}} \cdot 100 \tag{4}$$

where C_T is the capacitance over a temperature range, and C_{RT} is the capacitance value at RT. It is important

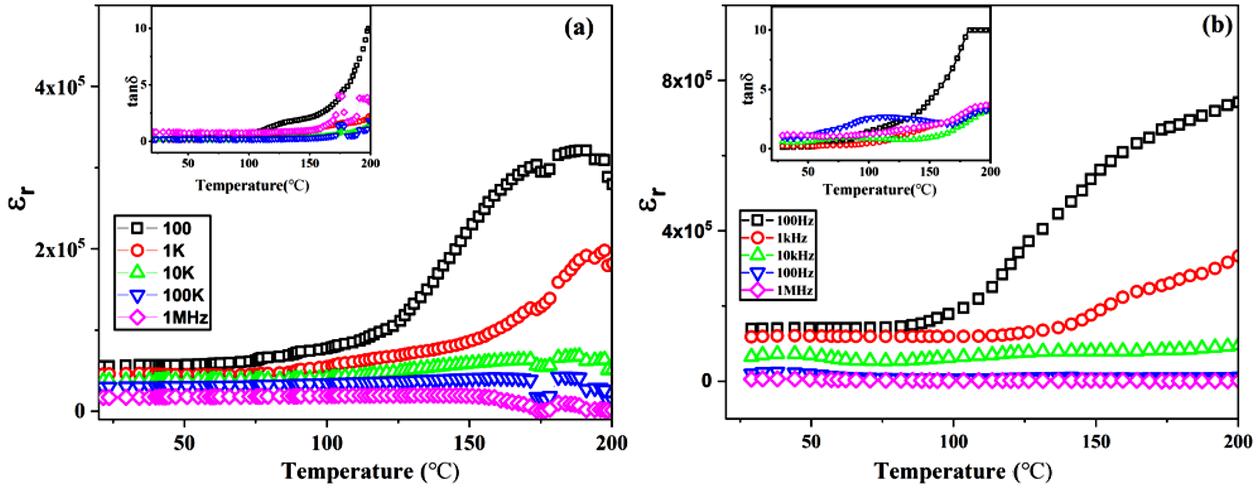

Figure 8. Variation of ε_r and tan δ with temperature at different frequencies of: a) CCTO-1050 and b) CCTO-1100 ceramics

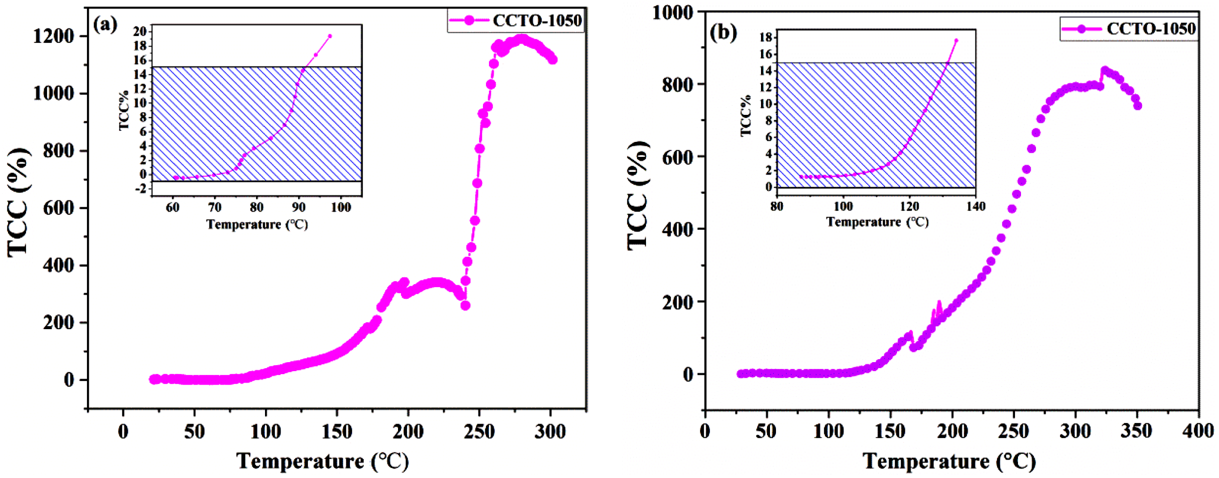

Figure 9. Variations of *TCC* (%) with temperature at 1 kHz for: a) CCTO-1050 and b) CCTO-1100 ceramics

to note that the *TCC* value should be less than ±15% for EIA code capacitors' applications [2].

Figures 9a and 9b demonstrate that the *TCC* value lies within ±15% in the temperature range up to 94 °C and 134 °C for the CCTO-1050 and CCTO-1100 ceramics, respectively, at 1 kHz frequency. Excellent dielectric properties along with low *TCC* compared to earlier reports on CCTO system makes the CCTO-1100 ceramics suitable candidate for electronic device applications.

IV. Conclusions

$CaCu_3Ti_4O_{12}$ (CCTO) ceramics were prepared by solid-state reaction route, calcination at 1050 °C for 4 h and sintering at 1050 and 1100 °C for 8 h. Effect of sintering temperature on microstructure and dielectric properties of the CCTO system was studied in detail. Dense microstructure was obtained in the CCTO-1100 ceramics sintered at 1100 °C. A giant ε_r of $\sim 14 \cdot 10^5$ with low $\tan\delta$ value at 100 Hz and at RT was observed in the CCTO-1100 ceramic sample. Accumulation of CuO melted phase around the grain boundary regions was accounted for the increase of ε_r. Excellent dielectric properties along with low *TCC* makes the CCTO-1100 ceramic sample useful candidate for electronic device applications.

References

1. D.C. Sinclair, T.B. Adams, F.D. Morrison, A.R. West, "$CaCu_3Ti_4O_{12}$: One-step internal barrier layer capacitor", *Appl. Phys. Lett.*, **80** (2002) 2153–2155.
2. P. Mao, J. Wang, L. Zhang, S. Liu, Y. Zhao, Q. Sun, "Rapid fabrication and improved electrical properties of $CaCu_3Ti_4O_{12}$ ceramics by sol-gel and spark plasma sintering techniques", *J. Mater. Sci. Mater. Electro.*, **30** (2019) 13401–13411.
3. M. Ahmadipour, M.F. Ain, Z.A. Ahmad "A Short review on copper calcium titanate (CCTO) electroceramic: Synthesis, dielectric properties, film deposition, and sensing application", *Nano-Micro Lett.*, **8** [4] (2016) 291–311.
4. W. Li, R.W. Schwartz, "Maxwell-Wagner relaxations and their contributions to the high permittivity of calcium copper titanate ceramics", *Phys. Rev. B*, **75** (2007) 012104.
5. X. Huang, Y. Jiang, K. Wu, "CCTO giant dielectric ceramic prepared by reaction sintering", *Procedia Eng.*, **102** (2015) 468–474.
6. Y. Yan, L. Jin, L. Feng, G. Cao, "Decrease of dielectric loss in giant dielectric constant $CaCu_3Ti_4O_{12}$ ceramics by adding $CaTiO_3$", *Mater. Sci. Eng. B*, **130** (2006) 146–150.
7. S. Jesurani, S. Kanagesan, R. Velmurugan, T. Kalaivani, "Phase formation and high dielectric constant of calcium copper titanate using sol-gel route", *J. Mater. Sci. Mater. Electro.*, **23** (2012) 668–674.
8. P. Mao, J. Wang, S. Liu, L. Zhang, Y. Zhao, L. He, "Grain size effect on the dielectric and non-ohmic properties of $CaCu_3Ti_4O_{12}$ ceramics prepared by the sol-gel process", *J. Alloys Compd.*, **778** (2019) 625–632.
9. J. Zhao, M. Chen, Q. Tan, "Embedding nanostructure and colossal permittivity of TiO_2-covered CCTO perovskite materials by a hydrothermal route", *J. Alloys Compd.*, **885** (2021) 160948.
10. Y. Qiu, Z.J. Zou, L.H. Zhou, M.R. Bai, X.H. Li, "Microstructure, dielectric and nonlinear electrical properties associated with sintering conditions in calcium copper titanate ceramics", *J. Mater. Sci. Mater. Electro.*, **28** (2017) 11091–11097.
11. D. Valim, A.G. Souza Filho, P.T.C. Freire, S.B. Fagan, A.P. Ayala, J. Mendes Filho, A.F.L. Almeida, P.B.A. Fechine, A.S.B. Sombra, J. Staun Olsen, L. Gerward, "Raman scattering and x-ray diffraction studies of polycrystalline $CaCu_3Ti_4O_{12}$ under high-pressure", *Phys. Rev. B*, **70** (2004) 2–5.
12. N. Kolev, R.P. Bontchev, A.J. Jacobson, V.N. Popov, V.G. Hadjiev, A.P. Litvinchuk, M.N. Iliev, "Raman spectroscopy of $CaCu_3Ti_4O_{12}$", *Phys. Rev. B*, **66** (2002) 132102.
13. R. Schmidt, M.C. Stennett, N.C. Hyatt, J. Pokorny, J. Prado-Gonjal, M. Li, D.C. Sinclair, "Effects of sintering temperature on the internal barrier layer capacitor (IBLC) structure in $CaCu_3Ti_4O_{12}$ (CCTO) ceramics", *J. Eur. Ceram. Soc.*, **32** (2012) 3313–3323.
14. V. Puli, S. Adireddy, M. Kothakonda, R. Elupula, D.B. Chrisey, "Low temperature sintered giant dielectric permittivity $CaCu_3Ti_4O_{12}$ sol-gel synthesized nanoparticle capacitors", *J. Adv. Dielectr.*, **7** (2017) 1750017.

15. P.S. Murthy, V.P. Venugopalan, D.D. Arunya, S. Dhara, R. Pandiyan, A.K. Tyagi, "Antibiofilm activity of nano sized CuO", pp. 580–583 in *International Conference on Nanoscience, Engineering and Technology* (ICONSET), IEEE Chennai, India, 2011.
16. J.J. Romero, P. Leret, F. Rubio-Marcos, A. Quesada, J.F. Fernández, "Evolution of the intergranular phase during sintering of $CaCu_3Ti_4O_{12}$ ceramics", *J. Eur. Ceram. Soc.*, **30** (2010) 737–742.
17. J. Zhang, Z. Li, Y. Liu, J. Zheng, W. Lu, S. Guo, Z. Lei, L. Lin, M. Tian, "Enhanced dielectric properties of CCTO ceramics doped by different halogen elements", *J. Mater. Sci. Mater. Electro.*, **31** (2020) 8481–8488.
18. R.R. Negi, M. Chandrasekhar, P. Kumar, "Structural, microstructural, dielectric and ferroelectric properties of $BaTiO_3$-based ceramics", *Process. Appl. Ceram.*, **13** (2019) 164–172.
19. B. Khumpaitool, J. Khemprasit, "Improvement in dielectric properties of Al_2O_3-doped $Li_{0.30}Cr_{0.02}Ni_{0.68}O$ ceramics", *Mater. Lett.*, **65** (2011) 1053–1056.
20. K. Lee, J. Kim, "Frequency and temperature dependence of the dielectric properties of a PCB substrate for advanced packaging applications", *J. Korean Phys. Soc.*, **54** (2009) 1096–1099.